HHS Public Access

Author manuscript

Sci Transl Med. Author manuscript; available in PMC 2019 February 08.

Published in final edited form as:

Sci Transl Med. 2017 January 11; 9(372): . doi:10.1126/scitranslmed.aai8269.

Targeting Aurora kinase A and JAK2 prevents GVHD while maintaining T_{reg} and antitumor CTL function

Brian C. Betts[1,2,3,*], **Anandharaman Veerapathran**[1,2], **Joseph Pidala**[1,2,3], **Hua Yang**[3], **Pedro Horna**[3,4], **Kelly Walton**[2], **Christopher L. Cubitt**[5], **Steven Gunawan**[3], **Harshani R. Lawrence**[3,6], **Nicholas J. Lawrence**[3,6], **Said M. Sebti**[3,6], and **Claudio Anasetti**[1,2,3]

[1]Department of Blood and Marrow Transplantation, Moffitt Cancer Center, Tampa, FL 33612, USA

[2]Department of Immunology, Moffitt Cancer Center, Tampa, FL 33612, USA

[3]Department of Oncologic Sciences, University of South Florida, Tampa, FL 33612, USA

[4]Department of Hematopathology and Laboratory Medicine, Moffitt Cancer Center, Tampa, FL 33612, USA

[5]Translational Research Core, Moffitt Cancer Center, Tampa, FL 33612, USA

[6]Department of Drug Discovery, Moffitt Cancer Center, Tampa, FL 33612, USA

Abstract

Graft-versus-host disease (GVHD) is a leading cause of nonrelapse mortality after allogeneic hematopoietic cell transplantation. T cell costimulation by CD28 contributes to GVHD, but prevention is incomplete when targeting CD28, downstream mammalian target of rapamycin (mTOR), or Aurora A. Likewise, interleukin-6 (IL-6)–mediated Janus kinase 2 (JAK2) signaling promotes alloreactivity, yet JAK2 inhibition does not eliminate GVHD. We provide evidence that blocking Aurora A and JAK2 in human T cells is synergistic in vitro, prevents xenogeneic GVHD, and maintains antitumor responses by cytotoxic T lymphocytes (CTLs). Aurora A/JAK2 inhibition is immunosuppressive but permits the differentiation of inducible regulatory T cells (iT_{regs}) that are hyperfunctional and CD39 bright and efficiently scavenge adenosine triphosphate (ATP). Increased iT_{reg} potency is primarily a function of Aurora A blockade, whereas JAK2 inhibition suppresses T helper 17 (T_H17) differentiation. Inhibiting either Aurora A or JAK2 significantly suppresses T_H1 T cells. However, CTL generated in vivo retains tumor-specific killing despite Aurora A/JAK2 blockade. Thus, inhibiting CD28 and IL-6 signal transduction pathways in donor T cells can increase the T_{reg}/T_{conv} ratio, prevent GVHD, and preserve antitumor CTL.

[*]Corresponding author. brian.betts@moffitt.org.

Author contributions: B.C.B. designed and performed experiments, analyzed and interpreted data, and wrote the manuscript. A.V. and K.W. performed experiments and edited the manuscript. J.P. and H.Y. discussed experimental design and edited the manuscript. P.H. assisted with in vivo experiments and edited the manuscript. C.L.C. performed experiments and edited the manuscript. S.G., H.R.L., and N.J.L. synthesized the AJI-100 and AJI-214, interpreted chemical analysis and stability of AJI-100 and AJI-214 [using ^{1}H nuclear magnetic resonance (NMR), ^{13}C NMR high-performance liquid chromatography (HPLC)–mass spectrometry, and HPLC], and edited the manuscript. S.M.S. and C.A. designed experiments and edited the manuscript.

Competing interests: S.M.S., N.J.L., and H.R.L. hold a patent (US9249124) related to the synthesis and use of AJI-214 and AJI-100. B.C.B., J.P., S.M.S., N.J.L., H.R.L., and C.A. hold a provisional patent related to the use of AJI-214 and AJI-100 in GVHD prevention. Neither the inventors nor the Moffitt Cancer Center has received payment related to claims described in the patents. The other authors declare that they have no competing interests.

INTRODUCTION

Graft-versus-host disease (GVHD) is a leading cause of nonrelapse mortality after allogeneic hematopoietic cell transplantation (alloHCT). Broadly acting calcineurin inhibitors (CNIs) are often used to prevent GVHD but exert undesirable antagonistic effects on T cell receptor (TCR) signaling and regulatory T cell (T_{reg}) differentiation and function (1–3). The lack of immune selectivity by CNIs places the alloHCT recipient at risk for opportunistic infections and relapse of their underlying hematologic malignancy. As opposed to heavily impairing signal 1 (TCR signaling) of T cell activation with CNIs, GVHD may be prevented by targeting activation signal 2 (costimulation) and signal 3 (cytokine activation). Therefore, an alternative approach at GVHD prophylaxis is to concurrently target CD28 costimulation and interleukin-6 (IL-6) receptor activation of T cells by inhibiting key signal transduction molecules in these pathways.

CD28 costimulation contributes to T cell alloreactivity and GVHD. Rodent bone marrow transplant recipients receiving $CD28^-$ T cells experience much less GVHD, compared to wild-type T cells (4, 5). Blockade of ligand interactions between CD80/CD86 and CD28 with neutralizing antibody also reduces murine GVHD (4, 5). CD28 signal transduction activates mTOR and Aurora kinase in T cells (6). mTOR is a known pharmacologic target in GVHD prophylaxis (7–9), and its blockade is selectively toxic to conventional T cells (T_{conv}) compared to T_{reg} (10). When tacrolimus is omitted by design, sirolimus alone is inadequate because most treated patients develop grade II to IV acute GVHD 15 days after transplant (11). Aurora kinase isoforms ubiquitously regulate mitotic progression and cellular polarity in human cells (12, 13) but also mediate T cell costimulation (6). Aurora kinase can active substrates required for T cell proliferation that are shared with mTOR and is only partially curtailed by sirolimus (6). Complete inhibition of Aurora activity requires direct blockade of the molecule or targeting upstream phosphatidylinositol-3-OH kinase (6). Increased Aurora kinase A expression was recently correlated with acute GVHD in human recipients of alloHCT and in experimental models studying murine and nonhuman primate hosts (14). Moreover, pharmacologic blockade of this novel pathway with alisertib, an Aurora kinase A inhibitor, significantly delayed the onset of GVHD in mice (14). These data revealed that Aurora kinase A is biologically relevant to GVHD, but its inhibition alone does not fully control alloreactivity (14).

IL-6 receptor signaling polarizes T helper 1 (T_H1) and T_H17 cells that are effectors in GVHD and impairs T_{regs} that modulate GVHD (15–19). IL-6 activates Janus kinase 2 (JAK2) and leads to downstream phosphorylation of signal transducer and activator of transcription 3 (STAT3) (15, 16, 20). We observed that $CD4^+$ T cell JAK2 activity is increased among alloHCT recipients who later develop GVHD (21). Anti–IL-6 receptor antibody combined with a CNI ameliorates human GVHD (22), but it does not influence T_H1, T_H17, or T_{reg} differentiation (20, 22). JAK2 inhibition conversely polarizes human natural T_{reg} responses and inhibits T_H1 and T_H17 development in vitro (15). However, selective blockade of JAK2 alone does not provide lasting protection in murine GVHD (17). This observation is distinct from JAK1/JAK2 inhibition, where coblockade of JAK1 acts broadly to reduce GVHD (23) as well as beneficial antiviral cytotoxic T lymphocyte (CTL)

(24, 25). These data show that JAK2 activation contributes to GVHD, though its selective inhibition is insufficient to completely prevent GVHD, despite preservation of T_{regs}.

Given that CD28 costimulation and IL-6 signal transduction facilitate T cell activation after encountering alloantigen, we hypothesized that combined inhibition of Aurora kinase A and JAK2 signaling would cooperatively suppress alloreactivity. Moreover, we expected CTL responses to remain intact because the TCR and JAK1 are left unperturbed. Using human in vitro and xenogeneic GVHD experiments, we investigate how these independent cellular pathways significantly affect donor T cell activation, differentiation, and function. Our data support the concept that GVHD prevention can be accomplished by targeting Aurora kinase A and JAK2 without impairing T_{reg} or antitumor CTL function.

RESULTS

Synergistic immunosuppression is attainable with combined inhibition of Aurora kinase A and JAK2

Allogeneic mixed leukocyte reactions (alloMLRs) are standard assays used to assess human T cell proliferation against polyclonal or antigen-specific stimuli. In alloMLRs consisting of human T cells and allogeneic monocyte-derived dendritic cells (DCs), the JAK2 inhibitor TG101348 (26) reduced alloreactive T cell proliferation at concentrations of 350 nM and greater as previously reported (Fig. 1A) (15). The Aurora kinase A inhibitor alisertib (27, 28) suppressed the proliferative response of T cells in alloMLRs with a median inhibitory concentration (IC_{50}) of 10 μM (Fig. 1A). Synergistic suppression of T cells allostimulated by DCs was achieved when TG101348 and alisertib were added together at a ratio of 1:5, respectively, with a calculated combination index (CI) of <1 using the Chou-Talalay method (Fig. 1A) (29). The observed IC_{50} of the combination correlated with 350 nM TG101348 and 1.75 μM alisertib (Fig. 1A).

The chemical analogs AJI-214 and AJI-100 were designed and synthesized at the Moffitt Cancer Center (28, 30) and shown to inhibit Aurora kinase A and JAK2 with similar potency (figs. S1 and S2). AJI-100 differs from AJI-214 by a single chlorine to hydrogen substitution at the ortho position of its phenyl ring, enhancing its solubility (28, 30), hence its preferred use in vivo (Fig. 1, B and C). Because AJI-100 is tolerated in mouse models (28), we performed a kinase target screen on AJI-100 to verify its activity against Aurora kinase A and JAK2 among a panel of 140 kinases (fig. S2). Aurora kinase A and JAK2 were among the top three kinases inhibited by AJI-100. We found that AJI-100 also inhibits 5′ AMP-activated protein kinase (AMPK) and exhibits slightly more potent suppression of Aurora kinase B than alisertib (fig. S2) (31).

AJI-214 and AJI-100 exerted significant suppression of T cells in alloMLRs, with single-agent efficacy at nanomolar concentrations ($P < 0.05$; Fig. 1, B and C). Moreover, the AJI analogs suppressed alloreactive T cell proliferation similar to the potency of alisertib (1.75 μM) and TG101348 (350 nM) combined (Fig. 1D). AJI-214 and AJI-100 (750 nM for each) also exhibited similar target inhibition of Aurora kinase A and JAK2 signal transduction in human T cells, reducing the phosphorylation of histone 3 serine 10 ($pH3Ser^{10}$) and STAT3

(pSTAT3) Y705, respectively (Fig. 1, E to H). As expected, alisertib only inhibited pH3Ser^{10} (Fig. 1, E and F), and TG101348 only inhibited pSTAT3 (Fig. 1, G and H).

Concurrent blockade of Aurora kinase A and JAK2 is immunosuppressive and permits the differentiation of inducible T_{reg}

DMSO, alisertib, TG101348, a combination of alisertib and TG101348, AJI-214, or AJI-100 was added to allogeneic cocultures of DC-stimulated T cells. Activated $CD4^+$ T_{conv} were identified as coexpressing CD25 and CD127 (32–34), and the latter assisted in excluding T_{regs} from the analysis (35, 36). CD25 expression alone was used to identify activated $CD8^+$ T_{conv}. Although all inhibitors suppressed the activated T_{conv} compared to DMSO, combined inhibition of Aurora A and JAK2 offered greater immunosuppression than either alisertib ($P = 0.007$, Fig. 2A; $P = 0.002$, Fig. 2B) or TG101348 alone ($P = 0.02$, Fig. 2A; $P = 0.02$, Fig. 2B). To quantify the effect of Aurora A/JAK2 blockade on T_H17, we performed IL-17 ELISPOTs using DC-stimulated, purified $CD4^+$ T cells in the presence of the compounds or DMSO. As predicted by the effect of each inhibitor on STAT3 phosphorylation, the JAK2-targeting compounds significantly reduced T_H17, whereas alisertib had no effect ($P < 0.05$; Fig. 2C). All of the inhibitors significantly decreased the frequency of interferon-γ^+ (IFN-γ^+) T_H1 T cells among treated allogeneic cocultures ($P < 0.05$; Fig. 2D). However, dual blockade of Aurora A and JAK2 did not offer increased suppression of T_H1 compared to either inhibitor alone (Fig. 2D).

Given that inhibition of Aurora A and JAK2 significantly reduced alloreactive T_{conv}, T_H1, and T_H17 cells, we then studied the effects of dual blockade on inducible T_{reg} (iT_{reg}) differentiation. Naïve $CD4^+$ T cells (>99% pure; Fig. 2E) were depleted of natural T_{regs} and stimulated with allogeneic DCs for 5 days in the presence of DMSO, alisertib, TG101348, a combination of alisertib and TG101348, AJI-214, or AJI-100. The iT_{regs} were identified as $CD4^+$, $CD127^-$, $CD25^+$, and $Foxp3^+$ (35, 36). iT_{reg} conversion from naïve $CD4^+$ precursors was variably reduced by all of the compounds compared to DMSO (Fig. 2, F and G), and Aurora A inhibition appeared to exert greater iT_{reg} impairment than JAK2 inhibition (Fig. 2G). In contrast, IL-2–induced STAT5 phosphorylation, which is required for T_{reg} development, remained intact among T cells treated with alisertib, TG101348, a combination of alisertib and TG101348, or the AJI analogs compared to DMSO (Fig. 2H).

Dual inhibition of Aurora kinase A and JAK2 supports potent $CD39^+$ iT_{reg}

We confirmed that AJI-214 and AJI-100 exhibit identical suppressive potency in regard to Aurora A and JAK2 signal transduction and human T cell proliferation assays. Therefore, we used AJI-214 as the representative bispecific analog for additional iT_{reg}-based in vitro mechanistic tests. Given that iT_{regs} are derived from phenotypically plastic naïve $CD4^+$ T cells, we confirmed that demethylated Foxp3 T_{reg}-specific demethylated region (TSDR) was similar among AJI-214–exposed and DMSO-exposed iT_{regs} (Fig. 3A). To study the influence of dual pathway inhibition on iT_{reg}-suppressive function, we cultured AJI-214–treated or DMSO-treated iT_{reg} with autologous T cells targeting fresh allogeneic DCs. The AJI-214–treated iT_{regs} demonstrated intact suppressive function, and its potency was significantly increased by about 30% compared to DMSO-treated iT_{regs} ($P = 0.018$; Fig. 3B). We then explored how Aurora kinase A versus JAK2 blockade contributed to this

enhanced suppression by the iT_{regs}. Antigen-specific iT_{regs} were generated from CD25-depleted $CD4^+$ T cells in the presence of alisertib, TG101348, a combination of alisertib and TG101348, or DMSO. Aurora kinase A inhibition with alisertib demonstrated superior suppressive capacity compared with either DMSO-exposed ($P = 0.03$) or TG101348-exposed ($P = 0.04$) iT_{reg} (Fig. 3C). The combination of alisertib with TG101348 was similar to alisertib alone (Fig. 3C).

We investigated the mechanism supporting the increased iT_{reg} function observed with AJI-214. We identified a significant increase in the cell surface density of CD39, an ectonucleotidase that hydrolyzes adenosine triphosphate (ATP), among the AJI-214–exposed iT_{reg} compared with DMSO controls ($P = 0.045$; Fig. 4, A to D). As reported by others, CD39 expression on non-T_{reg} $CD4^+$ T cells was minimal (Fig. 4, B to D) (37). We confirmed that the higher CD39 cell surface density among the AJI-214–treated iT_{regs} resulted in improved scavenging of extracellular ATP, compared to DMSO-treated iT_{regs} (Fig. 4E). The enhanced hydrolysis of ATP by the AJI-214–treated iT_{regs} was also significantly impaired by blocking the CD39 enzyme with ARL67156 ($P < 0.0001$; Fig. 4E). To determine the influence of $CD39^+$ iT_{reg} in the overall efficacy of dual Aurora A/JAK2 blockade, we added ARL67156 to alloMLRs consisting of natural T_{reg}-depleted $CD4^+$ T cell responders with AJI-214 or DMSO. This eliminated potential interference from $CD39^+$ natural T_{reg} within the allogeneic coculture and ensured that the only T_{regs} present in the system were induced. Moreover, ARL67156 would primarily affect the iT_{reg} as T_{conv} express negligible amounts of CD39. CD39 blockade significantly weakened the T cell inhibition by AJI-214 ($P = 0.037$; Fig. 4F), supporting that $CD39^+$ iT_{regs} contribute to the immunosuppressive effects of AJI-214. With regard to other modes of iT_{reg} suppression, we did not find any difference in their expression of LAG3 and CTLA4 or production of IL-10 or transforming growth factor–β (TGF-β) after exposure to AJI-214 or DMSO (Fig. 4, G to J).

Targeting Aurora kinase A and JAK2 reduces xenogeneic GVHD and preserves the generation antitumor CTL

A xenogeneic GVHD model was used to investigate the in vivo efficacy of dual Aurora kinase A/JAK2 blockade to specifically evaluate effects on human immune responses. Recipient NOD (nonobese diabetic) *scid* γ (NSG) mice were transplanted with human peripheral blood mononuclear cells (PBMCs) (30×10^6 cells) intraperitoneally (ip) on day 0. Independent donors were used for each experiment. We tested whether combining individual inhibitors of Aurora A and JAK2 prevented acute xenogeneic GVHD. Mice received alisertib (30 mg/kg daily), TG101348 (45 mg/kg twice a day), a combination of alisertib and TG101348, or methylcellulose vehicle from days 0 to +14 by oral gavage. The drug combination significantly delayed the onset and severity of GVHD, compared to vehicle or TG101348 alone ($P < 0.0001$ and $P = 0.0001$, respectively; Fig. 5, A and B). There was also a suggestion toward an improved median survival with the drug combination compared to alisertib (50.5 versus 41 days; P = not significant).

The bispecific inhibitor AJI-100 was used to test the in vivo efficacy of single-agent blockade of Aurora A and JAK2 as GVHD prevention. As demonstrated, AJI-100 offers

identical on-target inhibition and immunosuppressive properties as AJI-214 but exhibits superior bio-availability (28, 30). Compared to using the combination of alisertib and TG101348, AJI-100 had the advantage of being given once daily by intraperitoneal injection and avoided the need for sustained gavage dosing. Additionally, the single bispecific compound provided a pharmacologically cleaner approach by eliminating the variability in pharmacokinetics between the two drugs in combination. The recipient mice were transplanted with human cell as described. AJI-100 (50 mg/kg) or vehicle control was administered daily by intraperitoneal injection from days 0 to +14. AJI-100 significantly improved the overall survival of the mice and reduced the severity of GVHD, compared to vehicle control ($P = 0.003$; Fig. 5, C and D). On-target inhibition of Aurora A and JAK2 was confirmed among human T cells harvested from recipient spleens at day +14. AJI-100 significantly reduced the amount of $pH3Ser^{10+}$ and $pSTAT3^{+}$ T cells, respectively ($P = 0.027$ and $P = 0.0098$, respectively; Fig. 5, E and F).

We used an established method to generate human antitumor CTL in vivo and then test their specific killing (38, 39). $CD8^{+}$ CTLs were generated in xenotrans-planted mice receiving AJI-100 or vehicle control, where an inoculum of irradiated U937 cells was administered on day 0 and day +7. Unvaccinated, xenotrans-planted mice served as negative control. Despite its immunosuppressive activity, AJI-100 did not inhibit CTL generation because $CD8^{+}$ CTL from AJI-100–treated and vehicle-treated mice demonstrated similarly enhanced killing capacity against U937 targets in vitro, compared to unvaccinated controls (Fig. 5G). These data support that although AJI-100 significantly reduces GVHD, it also preserves anti-tumor CTL responses.

AJI-100 significantly increases the ratio of T_{reg} to activated T_{conv} while eliminating T_H17 and T_H1 T cells

Similar to its activity in vitro, AJI-100 suppressed the in vivo expansion of human T cells in the xenotransplanted mice. The absolute number of total $CD4^{+}$ T cells ($P < 0.0001$), T_{regs} ($P = 0.001$), and activated $CD4^{+}$ T_{conv} ($P < 0.0001$) from recipient spleens at day +14 was all significantly reduced by AJI-100 compared to vehicle (Fig. 6, A to E). Activated T_{conv} were proportionally more reduced by AJI-100 compared to T_{reg} (Fig. 6, B and C). Therefore, the ratio of T_{reg} to activated T_{conv} was significantly increased among mice treated with AJI-100 compared to vehicle ($P = 0.034$; Fig. 6D). AJI-100 also significantly reduced the amount of spleen-resident human T_H17 and T_H1 T cells, compared to vehicle ($P = 0.002$ for both; Fig. 6, F to H). AJI-100 also exerted a suppressive effect on $CD8^{+}$ T cell and $CD19^{+}$ B cell reconstitution as determined by absolute numbers compared to vehicle (fig. S3, A to F). However, the frequencies of $CD4^{+}$ and $CD8^{+}$ T cells and $CD19^{+}$ B cells were similar among AJI-100–treated and vehicle-treated mice (fig. S3, C, D, and F). The primary host target organs affected by GVHD at day +14 in this xenogeneic model were liver and lung. GVHD severity within these organs was significantly reduced by AJI-100, compared to vehicle ($P = 0.043$ and $P = 0.002$, respectively; Fig. 6, I to K). Immunohistochemistry demonstrated that the number of tissue-infiltrating, human $CD3^{+}$ T cells in recipient liver and lung was also significantly decreased by AJI-100 treatment ($P = 0.006$ and $P = 0.002$, respectively; Fig. 6, L and M).

DISCUSSION

T cell costimulation and cytokine activation independently contribute to GVHD, but control of donor alloresponses is incomplete when targeting either pathway alone (5, 14, 15, 17). Here, we demonstrate that GVHD prevention can be accomplished by dual inhibition of Aurora kinase A and JAK2, attenuating CD28 costimulation (6) and IL-6–mediated signal transduction, respectively, without ablating potential antitumor CTL responses (15, 16, 21). Concurrent blockade of Aurora kinase A and JAK2 yields synergistic immunosuppression of human allogeneic T cells in vitro, significantly enhances iT_{reg}-suppressive potency, and enhances the ratio of T_{regs} to activated T_{conv} in vivo. These characteristics are distinct from CNI-based GVHD prophylaxis, which inhibits TCR function and indiscriminately suppresses donor T cells (1–3). The lack of selectivity by CNIs results in a failure to achieve donor immune tolerance toward the host and mitigates the graft-versus-leukemia (GVL) potential of the allograft (1–3).

Inhibition of Aurora kinase A or JAK2 activity individually suppressed human T cell proliferation in alloMLRs, and synergy was achieved in vitro with simultaneous blockade of both signal transduction pathways. We used a xenogeneic model to study human T cell responses in vivo after Aurora kinase A and JAK2 blockade, understanding that the lack of recipient conditioning does differ from clinical practice in allogeneic HCT. We show that alisertib combined with TG101348 significantly delays GVHD. However, the combination of inhibitors appears additive at best in vivo and does not completely eliminate GVHD. The bispecific inhibitor AJI-100 significantly reduced GVHD and improved survival compared to vehicle control. We surmise that the apparent enhanced in vivo activity of AJI-100 compared to alisertib plus TG101348 may be due to inherent kinase selectivity. The ratio of Aurora kinase A to kinase B inhibition by AJI-100 is greater than alisertib (fig. S2) (31). This could contribute to enhanced impairment of T cell costimulation by AJI-100 and secondarily enhance efficacy (6). Although the role of AMPK in GVHD is unknown, mouse models of inflammatory colitis using AMPK-deficient T cells suggest that AMPK neutralization may have immunosuppressive properties as well (40). Therefore, off-target inhibition of AMPK by AJI-100 could be beneficial in controlling GVHD. However, the immunosuppressive effects of the combination of the JAK2 inhibitor TG101348 and the Aurora kinase A inhibitor alisertib coupled with the potent activity of AJI-100 suggests that the ability of AJI-100 to prevent GVHD is likely due to its dual JAK2/Aurora kinase A inhibitory activity.

Blockade of Aurora kinase A or JAK2 induces pathway-specific effects on developing iT_{reg} and T_H17. First, blockade of Aurora kinase A and JAK2 permits the differentiation of highly suppressive, alloantigen-specific, $CD39^+$ iT_{reg}. Patients with rheumatoid arthritis lacking sufficient $CD39^+$ T_{regs} experience greater rates of methotrexate failure and poor clinical outcomes (41, 42), suggesting that dual Aurora kinase A/JAK2 inhibition may benefit other inflammatory conditions. Our data support that the enhanced iT_{reg} potency is largely a function of Aurora kinase A inhibition because iT_{regs} exposed to alisertib, an Aurora kinase A–specific inhibitor, eliminated T_{conv} proliferation. On the other hand, alisertib was unable to prevent T_H17 differentiation among naïve $CD4^+$ T cells responding to alloantigen. Given that IL-6 receptor signal transduction facilitates T_H17 development (15, 18), our data

confirm that JAK2 blockade is capable of restraining STAT3 phosphorylation and resultant T_H17 differentiation. Additionally, JAK2 inhibition appears to exhibit less inhibition of iT_{regs} compared to Aurora kinase A blockade. Last, inhibition of JAK2, Aurora kinase A, or both JAK2 and Aurora kinase A equally impaired the T_H1 response in vitro.

Selective inhibition of Aurora kinase A and JAK2 paired with preserved common gamma-chain cytokine signaling establishes a platform to control alloreactivity while permitting antigen-specific T_{reg} and CTL responses. However, there are several limitations of this study that deserve further consideration. Although the xenogeneic model is well suited to test whether concurrent Aurora kinase A/JAK2 inhibition can prevent GVHD mediated by human cells in vivo, it does not entirely replicate human GVHD pathogenesis. The recipient mice do not receive transplant conditioning, unlike human patients, and this may affect GVHD target-organ injury, host antigen presentation, and the production of relevant cytokines such as IL-6. Our work demonstrates that AJI-100 permits the generation and function of antitumor CTL, but it is important to recognize that such experiments are supportive and not definitive in assessing whether the bispecific inhibitor preserves GVL in vivo. Last, small-molecule inhibitors can exhibit off-target inhibition, as we observed with AJI-100 and its suppression of AMPK. Unlike molecular knockout strategies, off-target effects by pharmacologic inhibitors may be immunologically relevant and should be considered when interpreting such data.

CNI-free GVHD prophylaxis is an important concept in improving patient outcomes after clinical transplantation. The challenges of CNI-based GVHD prevention are clear because CNIs offer incomplete protection from severe GVHD and render the donor immune system poorly equipped to counter posttransplant relapse (1–3). Given that targeting Aurora kinase A and JAK2 significantly reduces activated T_{conv} while permitting T_{regs} and tumor-specific CTL, the concept described here may represent a translatable CNI-free approach at GVHD prevention. A limited number of CNI-free GVHD prophylaxis strategies currently exist and include T cell depletion of the allograft (43) or the use of posttransplant cyclophosphamide (44). The bispecific inhibitor AJI-100 is an attractive alternative because it does not require ex vivo allograft modification (43) or the need to expose freshly infused donor stem cells to potent alkylators (44). Hence, further investigation of dual Aurora kinase A/JAK2 inhibition is merited to promote selective control of donor immune responses after alloHCT.

MATERIALS AND METHODS

Study design

The first part of the study evaluated the in vitro effects of dual Aurora kinase A/JAK2 inhibition on human allostimulated T cells. This included a formal test for synergistic inhibition of T cell proliferation by combining alisertib (Aurora kinase A inhibitor) and TG101348 (JAK2 inhibitor) in standard alloMLRs. The Chou-Talalay method was used to calculate the CI and assess whether the drug combination was synergistic (<1), additive (equal to 1), or antagonistic (>1) (29). We went on to determine how Aurora kinase A and JAK2 signal transduction pathways contributed to human T cell activation and the differentiation of T_H1, T_H17, and iT_{regs} in vitro using a combination of alisertib and TG101348, as well as the bispecific inhibitors AJI-214 and AJI-100. We tested whether

concurrent blockade of Aurora kinase A and JAK2 led to enhanced iT_{reg}-suppressive potency both functionally and mechanistically, evaluating the effect of AJI-214 on iT_{reg} expression of CD39, LAG3, and CTLA4 and production of IL-10 and TGF-β. The second part of this study used a human/NSG mouse GVHD model to investigate whether dual Aurora kinase A/JAK2 blockade could prevent xenogeneic GVHD using a combination of alisertib and TG101348 or AJI-100 in separate sets of experiments. For GVHD experiments, the end point was premoribund state, and the mice were monitored frequently for GVHD clinical scores. Histopathologic scores were assessed on day +14 as indicated. Additionally, we investigated whether AJI-100 permitted the generation of U937-specific CTL in vivo and then tested the specific cytotoxicity of the CTL in vitro. All murine in vivo data were pooled from at least two independent experiments with $n = 6$ to 14 mice per group.

Allogeneic mixed leukocyte reactions

Healthy donor T cells were purified by nylon wool elution or magnetic bead separation and allostimulated with allogeneic DCs (DC/T cell ratio of 1:30) as previously described (OneBlood) (15, 16, 20). DCs were cytokine-matured with IL-1β, IL-6, tumor necrosis factor–α, and prostaglandin E_2 (15, 16, 20). For synergy assays, TG101348 (JAK2 inhibitor, Chemietek), alisertib (Aurora kinase A inhibitor, Selleckchem), or both TG101348 and alisertib (ratio of 1:5, respectively) were added once on day 0. Alisertib, TG101348, a combination of alisertib and TG101348, AJI-214, AJI-100 [dual JAK2 and Aurora kinase A inhibitors (28, 30), Moffitt Chemical Biology Core; fig. S1], or DMSO (<0.1%) was added once on day 0 at concentrations ranging from 0.078 to 2.5 μM. These experiments were performed twice with four technical replicates for each condition. Different DC/T cell donor pairs were used for each experiment. As indicated, we treated alloMLRs consisting of natural T_{reg}-depleted, naïve $CD4^+$ T cells (Miltenyi Biotec Inc) with a combination of ARL67156 (CD39 inhibitor, 125 μM; Sigma), AJI-214, and DMSO on day 0 to study the role of CD39 and ATP in this system. T cell proliferation was measured on day 5 by a colorimetric assay [CellTiter 96 AQ_{ueous} One Solution Cell Proliferation Assay [3-(4,5-dimethyl-2-yl)-5-(3-carboxymethoxyphenyl)-2-(4-sulfophenyl)-2H-tetrazolium, inner salt (MTS)] or CellTiter-Blue, Promega] (15, 16, 20). Absorbance or optical density (OD) was analyzed at 490 or 590 nm, respectively. Percent proliferation was calculated as follows: [(OD of treated alloMLR − OD of T cells alone)/(OD of DMSO alloMLR − OD of T cells alone)] × 100. These experiments were performed three to seven times as indicated with triplicate technical replicates for each condition. Different DC/T cell donor pairs were used for each experiment.

Monoclonal antibodies and flow cytometry

Fluorochrome-conjugated mouse anti-human monoclonal antibodies included anti-CD3, CD4, CD8, CD25, CD39, CD127, CTLA4, Foxp3, LAG3, pSTAT3 Y705, pSTAT5 Y694, and $pH3Ser^{10}$ (BD Biosciences, eBioscience, and Cell Signaling Technology). LIVE/DEAD Fixable Yellow Dead Cell Stain (Life Technologies) was used to determine viability. Live events were acquired on a FACSCanto or LSR II Flow Cytometer (FlowJo software, version 7.6.4; Tree Star).

Protein phosphorylation in T cells

H3Ser^{10} phosphorylation—T cells were cultured with allogeneic DCs (DC/T cell ratio of 1:30) for 5 days in RPMI/10% pooled human serum, with alisertib (1.75 μM), TG101348 (350 nM), a combination of both inhibitors, AJI-214 (750 nM), AJI-100 (750 nM), or DMSO control added once on day 0. After 5 days, T cells were then harvested and directly fixed (Cytofix, BD Biosciences) for 10 min at 37°C. After washing with phosphate-buffered saline, the T cells were permeabilized with ice-cold methanol (90%, v/v) for at least 20 min at −20°C. The cells were stained for expression of CD3 and pH3Ser^{10}.

STAT3 and STAT5 phosphorylation—As indicated, T cells were serum-starved in RPMI treated with DMSO diluent control, alisertib, TG101348, a combination of both inhibitors, AJI-214, or AJI-100 for 4 hours. IL-6–induced pSTAT3 or IL-2–induced pSTAT5 (Y694) was measured by flow cytometry as described (15, 16).

NSG mice—After transplantation and treatment with either AJI-100 or vehicle control, human T cells were isolated from recipient mouse spleens at day +14, stained for pH3Ser^{10} or pSTAT3 (+IL-6 stimulation), and analyzed as described.

Effect of dual pathway inhibition on effector CD4 T cell differentiation

Purified human T cells were allostimulated with DCs at a DC/T cell ratio of 1:30 in RPMI/10% pooled human serum. DMSO, alisertib (1.75 μM), TG101348 (350 nM), both alisertib and TG101348, AJI-214 (750 nM), or AJI-100 (750 nM) was added once on day 0. The T cells were harvested and surface-stained on day 5 for CD3, CD4, CD25, and CD127. Activated CD4$^+$ T_{conv} were characterized by expression of CD25 and CD127 (32–34), and activated CD8$^+$ T_{conv} (CD3$^+$ and CD4$^-$) were identified by CD25 expression. The absolute number of CD4$^+$ and CD8$^+$ T_{conv} was calculated by flow cytometry using CountBright beads (Life Technologies). T_H1 cells were characterized by expression of CD3, CD4, and intracellular IFN-γ (after an additional 4 to 5 hours of stimulation with PMA/ionomycin). For T_H1 experiments, purified CD4$^+$ T cells were used as opposed to bulk T cells.

iT$_{reg}$ differentiation and potency

iT_{regs} were generated as previously described (16) in the presence of alisertib (1.75 μM), TG101348 (350 nM), both alisertib and TG101348, AJI-214 (750 nM), AJI-100 (750 nM), or DMSO. On day 5, iT_{regs} were isolated and washed to minimize drug carry-over as reported (16). The T cells were harvested and surface-stained on day 5 for CD3, CD4, CD25, and CD127, followed by fixation and permeabilization (eBioscience) and Foxp3 staining (35, 36). The absolute number of iT_{reg} was calculated by flow cytometry using CountBright beads (Life Technologies). The purified iT_{regs} were titrated against alloMLRs consisting of responder CD4$^+$CD25$^-$ T cells (5×10^4) from the iT_{reg} donor and fresh allogeneic DCs (1.6×10^3) to determine suppressive potency. T cell proliferation was determined by pulsing cells with [^{3}H]thymidine (1 μCi per well) (16). Surface expression of CD39 and LAG3 was evaluated on the iT_{reg}. iT_{reg} production of CTLA4 was assessed by intracellular staining after a 5-hour treatment of PMA/ionomycin, with GolgiStop added during the last 4 hours of incubation. iT_{reg} synthesis of IL-10 and TGF-β (Quansys

Biosciences) was quantified from supernatants using multiplex cytokine assays after PMA/ionomycin stimulation.

ATP hydrolysis assay

iT_{reg} generated in the presence of AJI-214 (750 nM) or DMSO were plated in V-bottom 96-well plates in serum-free medium at a concentration of 75,000 cells/100 μl. ARL67156 (125 μM) was either added or not as indicated. A fixed dose of ATP (50 μM) was added to the cells and incubated at 37°C for 45 min. ATP consumption was measured by a luminescence assay according to the manufacturer's instructions (CellTiter-Glo Luminescent Cell Viability Assay, Promega) and was read by a spectrofluorometer. Percent consumption was calculated as follows: (luminescence of test supernatant/luminescence of 50 μM ATP cell-free control supernatant) × 100.

Foxp3 TSDR demethylation analysis

Foxp3 TSDR demethylation was analyzed among magnetic bead–purified (Miltenyi), allostimulated AJI-214–treated and DMSO-treated iT_{regs}. The primer selection, the procedure for amplifying methylation-specific and demethylation-specific TSDR products, genomic DNA isolation, bisulfite conversion, and quantitative polymerase chain reaction were performed as previously reported (16).

IL-17 ELISPOT

Naïve $CD4^+$ T cells were purified and allostimulated (DC/T cell ratio of 1:30) as reported (21). Alisertib (1.75 μM), TG101348 (350 nM), both alisertib and TG101348, AJI-214 (750 nM), AJI-100 (750 nM), or DMSO control was added once on day 0. Medium was supplemented with IL-6 (1×10^5 IU/ml), TGF-β (4 ng/ml; R&D Systems), and anti–IFN-γ monoclonal antibody (10 μg/ml; eBioscience) to polarize T_H17. After 5 days, the T cells were harvested, washed, and then plated at 35,000 cells per well in an IL-17 ELISPOT plate (R&D Systems). The $CD4^+$ T cells were stimulated with PMA/ionomycin, and the ELISPOT assay was performed according to the manufacturer's instructions. The resultant spots were read by a plate reader.

Xenogeneic GVHD model

NSG mice (6- to 24-week-old male or female) were purchased from The Jackson Laboratory and raised according to an Institutional Animal Care and Use Committee (IACUC)–approved protocol in adherence to the National Institutes of Health's *Guide for the Care and Use of Laboratory Animals*. Mice received fresh, human PBMCs (30×10^6 cells) ip from a uniform donor source (OneBlood) per experiment, once on day 0 of the transplant. Mice received either (i) alisertib (30 mg/kg daily), TG101348 (45 mg/kg twice a day), a combination of alisertib and TG101348, or vehicle (methylcellulose) by oral gavage or (ii) AJI-100 (50 mg/kg daily) or vehicle (50% polyethylene glycol, 15% 2-hydroxypropyl-β-cyclodextrin, and 10% DMSO in sterile saline) ip from day 0 to day +14. Mice were monitored for GVHD clinical scores (46), weight, and premoribund status. As indicated, mice were euthanized on day +14 to study recipient spleen T_{conv}, T_{regs}, T_H1, T_H17, B cells, and T cell signal transduction. Human T_{reg}, T_{conv}, T_H1, and $CD19^+$ B cells residing in

recipient spleens were quantified by flow cytometry. T cell pH3Ser^{10} and pSTAT3 were evaluated by flow cytometry. IL-17 ELISPOTs were performed using isolated human T cells from recipient mouse spleen as described above. Tissue samples were prepared, stained (Ventana Medical Systems), and imaged (Vista) to identify human T cells as previously described (21). GVHD pathology scores for recipient liver and lung were assigned in a standard fashion (45). All vertebrate animal work was IACUC-approved.

CTL generation and tumor lysis assays

NSG mice were transplanted with human PBMCs as described above and treated with either AJI-100 (50 mg/kg daily) or vehicle control. Additionally, recipient mice received an inoculum of irradiated U937 cells (1×10^7 per mouse; American Type Culture Collection) on days 0 and +7 (38, 39). Mice were euthanized between days +10 and +12, spleens were harvested, and human CD8$^+$ T cells were isolated by magnetic bead separation. Fresh U937 target cells were labeled with calcein-acetoxymethyl for 30 min, washed, and then cultured with the purified CD8$^+$ T cells at varying effector-to-target ratios for 4 hours at 37°C. No additional drugs were added during this final culture. The amount of supernatant fluorescence released by the target cells was measured using a spectrofluorometer (excitation at 485 nm and emission at 535 nm) (46). Percent lysis was calculated as follows: [(test fluorescence − spontaneous fluorescence)/(maximum fluorescence − spontaneous fluorescence)] × 100 (46).

Statistical analysis

For comparisons of paired data sets, the paired *t* test was used. ANOVA was used for group comparisons. Survival comparisons were made using the log-rank test. The Mann-Whitney test was used for all others. The statistical analysis was conducted using Prism software version 5.04 (GraphPad). Statistical significance was defined by $P < 0.05$ (two-tailed).

For drug combination experiments, the results were analyzed for synergistic, additive, or antagonistic effects using the CI method developed by Chou and Talalay (29). The dose-effect curve for each drug alone was determined on the basis of experimental observations using the median-effect principle and then compared to the effect achieved with a combination of the two drugs to derive a CI value. For this analysis, XLfit software (IDBS) was used to create log-log dose-fractional effect plots for each drug and combination and to regress a straight line through the points and was used to calculate the values of D_m and m for use in the median-effect equation as follows: $f_a/f_u = (D/D_m)m$, where D is the dose of the drug, D_m is the dose required for a 50% effect (analogous to IC_{50}), f_a and f_u are the affected and unaffected fractions, respectively ($f_a = 1 - f_u$), and m is the exponent signifying the sigmoidicity of the dose-effect curve. The CI calculation chosen for the analysis of the drug combinations was the isobologram equation for mutually nonexclusive drugs with different modes of action as follows: $CI = (D)_1/(Dx)_1 + (D)_2/(Dx)_2 + (D)_1(D)_2/(Dx)_1(Dx)_2$, where $(Dx)_1$ and $(Dx)_2$ in the denominators are the concentrations for drug 1 and drug 2 alone that gave x% inhibition, whereas $(D)_1$ and $(D)_2$ in the numerators are the concentrations of drug 1 and drug 2 in combination that also inhibited x% (that is, isoeffective).

Supplementary Material

Refer to Web version on PubMed Central for supplementary material.

Acknowledgments

We thank the Translational Research Core and Chemical Biology Core at the Moffitt Cancer Center and Research Institute for assisting with work performed in this article. The Department of Comparative Medicine, University of South Florida and the Flow Cytometry, Vivarium, Analytic Microscopy, and Tissue Cores at the Moffitt Cancer Center were also used in completing this work.

Funding: This work was supported by NIH grant K08 HL11654701A1 to B.C.B. The core facilities are partially supported by the Moffitt Cancer Center Support grant P30-CA076292.

REFERENCES AND NOTES

1. Vaeth M, Bäuerlein CA, Pusch T, Findeis J, Chopra M, Mottok A, Rosenwald A, Beilhack A, Berberich-Siebelt F. Selective NFAT targeting in T cells ameliorates GvHD while maintaining antitumor activity. Proc Natl Acad Sci USA. 112:1125–1130.2015; [PubMed: 25583478]
2. Singh K, Stempora L, Harvey RD, Kirk AD, Larsen CP, Blazar BR, Kean LS. Superiority of rapamycin over tacrolimus in preserving nonhuman primate Treg half-life and phenotype after adoptive transfer. Am J Transplant. 14:2691–2703.2014; [PubMed: 25359003]
3. Zeiser R, Nguyen VH, Beilhack A, Buess M, Schulz S, Baker J, Contag CH, Negrin RS. Inhibition of $CD4^+CD25^+$ regulatory T-cell function by calcineurin-dependent interleukin-2 production. Blood. 108:390–399.2006; [PubMed: 16522809]
4. Tan P, Anasetti C, Hansen JA, Melrose J, Brunvand M, Bradshaw J, Ledbetter JA, Linsley PS. Induction of alloantigen-specific hyporesponsiveness in human T lymphocytes by blocking interaction of CD28 with its natural ligand B7/BB1. J Exp Med. 177:165–173.1993; [PubMed: 7678111]
5. Yu XZ, Bidwell SJ, Martin PJ, Anasetti C. CD28-specific antibody prevents graft-versus-host disease in mice. J Immunol. 164:4564–4568.2000; [PubMed: 10779758]
6. Song J, Salek-Ardakani S, So T, Croft M. The kinases aurora B and mTOR regulate the G1-S cell cycle progression of T lymphocytes. Nat Immunol. 8:64–73.2007; [PubMed: 17128276]
7. Cutler C, Logan B, Nakamura R, Johnston L, Choi S, Porter D, Hogan WJ, Pasquini M, MacMillan ML, Hsu JW, Waller EK, Grupp S, McCarthy P, Wu J, Hu ZH, Carter SL, Horowitz MM, Antin JH. Tacrolimus/sirolimus vs tacrolimus/methotrexate as GVHD prophylaxis after matched, related donor allogeneic HCT. Blood. 124:1372–1377.2014; [PubMed: 24982504]
8. Pidala J, Kim J, Alsina M, Ayala E, Betts BC, Fernandez HF, Field T, Jim H, Kharfan-Dabaja MA, Locke FL, Mishra A, Nishihori T, Ochoa-Bayona L, Perez L, Riches M, Anasetti C. Prolonged sirolimus administration after allogeneic hematopoietic cell transplantation is associated with decreased risk for moderate-severe chronic graft-*versus*-host disease. Haematologica. 100:970–977.2015; [PubMed: 25840599]
9. Pidala J, Kim J, Jim H, Kharfan-Dabaja MA, Nishihori T, Fernandez HF, Tomblyn M, Perez L, Perkins J, Xu M, Janssen WE, Veerapathran A, Betts BC, Locke FL, Ayala E, Field T, Ochoa L, Alsina M, Anasetti C. A randomized phase II study to evaluate tacrolimus in combination with sirolimus or methotrexate after allogeneic hematopoietic cell transplantation. Haematologica. 97:1882–1889.2012; [PubMed: 22689677]
10. Zeiser R, Leveson-Gower DB, Zambricki EA, Kambham N, Beilhack A, Loh J, Hou JZ, Negrin RS. Differential impact of mammalian target of rapamycin inhibition on $CD4^+CD25^+Foxp3^+$ regulatory T cells compared with conventional $CD4^+$ T cells. Blood. 111:453–462.2008; [PubMed: 17967941]
11. Johnston L, Florek M, Armstrong R, McCune JS, Arai S, Brown J, Laport G, Lowsky R, Miklos D, Shizuru J, Sheehan K, Lavori P, Negrin R. Sirolimus and mycophenolate mofetil as GVHD prophylaxis in myeloablative, matched-related donor hematopoietic cell transplantation. Bone Marrow Transplant. 47:581–588.2012; [PubMed: 21552302]

12. Carmena M, Earnshaw WC. The cellular geography of aurora kinases. Nat Rev Mol Cell Biol. 4:842–854.2003; [PubMed: 14625535]
13. Lens SMA, Voest EE, Medema RH. Shared and separate functions of polo-like kinases and aurora kinases in cancer. Nat Rev Cancer. 10:825–841.2010; [PubMed: 21102634]
14. Furlan SN, Watkins B, Tkachev V, Flynn R, Cooley S, Ramakrishnan S, Singh K, Giver C, Hamby K, Stempora L, Garrett A, Chen J, Betz KM, Ziegler CGK, Tharp GK, Bosinger SE, Promislow DEL, Miller JS, Waller EK, Blazar BR, Kean LS. Transcriptome analysis of GVHD reveals aurora kinase A as a targetable pathway for disease prevention. Sci Transl Med. 7:315ra191.2015;
15. Betts BC, Abdel-Wahab O, Curran SA, St Angelo ET, Koppikar P, Heller G, Levine RL, Young JW. Janus kinase-2 inhibition induces durable tolerance to alloantigen by human dendritic cell-stimulated T cells yet preserves immunity to recall antigen. Blood. 118:5330–5339.2011; [PubMed: 21917753]
16. Betts BC, Veerapathran A, Pidala J, Yu XZ, Anasetti C. STAT5 polarization promotes iTregs and suppresses human T-cell alloresponses while preserving CTL capacity. J Leukoc Biol. 95:205–213.2014; [PubMed: 24068731]
17. Choi J, Cooper ML, Alahmari B, Ritchey J, Collins L, Holt M, DiPersio JF. Pharmacologic blockade of JAK1/JAK2 reduces GvHD and preserves the graft-versus-leukemia effect. PLOS ONE. 9:e109799.2014; [PubMed: 25289677]
18. Laurence A, Amarnath S, Mariotti J, Kim YC, Foley J, Eckhaus M, O'Shea JJ, Fowler DH. STAT3 transcription factor promotes instability of nTreg cells and limits generation of iTreg cells during acute murine graft-versus-host disease. Immunity. 37:209–222.2012; [PubMed: 22921119]
19. Zeiser R, Burchert A, Lengerke C, Verbeek M, Maas-Bauer K, Metzelder SK, Spoerl S, Ditschkowski M, Ecsedi M, Sockel K, Ayuk F, Ajib S, de Fontbrune FS, Na IK, Penter L, Holtick U, Wolf D, Schuler E, Meyer E, Apostolova P, Bertz H, Marks R, Lübbert M, Wäsch R, Scheid C, Stölzel F, Ordemann R, Bug G, Kobbe G, Negrin R, Brune M, Spyridonidis A, Schmitt-Gräff A, van der Velden W, Huls G, Mielke S, Grigoleit GU, Kuball J, Flynn R, Ihorst G, Du J, Blazar BR, Arnold R, Kröger N, Passweg J, Halter J, Socié G, Beelen D, Peschel C, Neubauer A, Finke J, Duyster J, von Bubnoff N. Ruxolitinib in corticosteroid-refractory graft-versus-host disease after allogeneic stem cell transplantation: A multi-center survey. Leukemia. 29:2062–2068.2015; [PubMed: 26228813]
20. Betts BC, St Angelo ET, Kennedy M, Young JW. Anti-IL6-receptor-alpha (tocilizumab) does not inhibit human monocyte-derived dendritic cell maturation or alloreactive T-cell responses. Blood. 118:5340–5343.2011; [PubMed: 21940820]
21. Betts BC, Sagatys EM, Veerapathran A, Lloyd MC, Beato F, Lawrence HR, Yue B, Kim J, Sebti SM, Anasetti C, Pidala J. $CD4^+$ T cell STAT3 phosphorylation precedes acute GVHD, and subsequent Th17 tissue invasion correlates with GVHD severity and therapeutic response. J Leukoc Biol. 97:807–819.2015; [PubMed: 25663681]
22. Kennedy GA, Varelias A, Vuckovic S, Le Texier L, Gartlan KH, Zhang P, Thomas G, Anderson L, Boyle G, Cloonan N, Leach J, Sturgeon E, Avery J, Olver SD, Lor M, Misra AK, Hutchins C, Morton AJ, Durrant STS, Subramoniapillai E, Butler JP, Curley CI, MacDonald KP, Tey SK, Hill GR. Addition of interleukin-6 inhibition with tocilizumab to standard graft-versus-host disease prophylaxis after allogeneic stem-cell transplantation: A phase 1/2 trial. Lancet Oncol. 15:1451–1459.2014; [PubMed: 25456364]
23. Spoerl S, Mathew NR, Bscheider M, Schmitt-Graeff A, Chen S, Mueller T, Verbeek M, Fischer J, Otten V, Schmickl M, Maas-Bauer K, Finke J, Peschel C, Duyster J, Poeck H, Zeiser R, von Bubnoff N. Activity of therapeutic JAK 1/2 blockade in graft-versus-host disease. Blood. 123:3832–3842.2014; [PubMed: 24711661]
24. Heine A, Brossart P, Wolf D. Ruxolitinib is a potent immunosuppressive compound: Is it time for anti-infective prophylaxis? Blood. 122:3843–3844.2013; [PubMed: 24288410]
25. Heine A, Held SAE, Daecke SN, Wallner S, Yajnanarayana SP, Kurts C, Wolf D, Brossart P. The JAK-inhibitor ruxolitinib impairs dendritic cell function in vitro and in vivo. Blood. 122:1192–1202.2013; [PubMed: 23770777]
26. Wernig G, Kharas MG, Okabe R, Moore SA, Leeman DS, Cullen DE, Gozo M, McDowell EP, Levine RL, Doukas J, Mak CC, Noronha G, Martin M, Ko YD, Lee BH, Soll RM, Tefferi A, Hood JD, Gilliland DG. Efficacy of TG101348, a selective JAK2 inhibitor, in treatment of a murine

model of JAK2V617F-induced polycythemia vera. Cancer Cell. 13:311–320.2008; [PubMed: 18394554]

27. Manfredi MG, Ecsedy JA, Chakravarty A, Silverman L, Zhang M, Hoar KM, Stroud SG, Chen W, Shinde V, Huck JJ, Wysong DR, Janowick DA, Hyer ML, Leroy PJ, Gershman RE, Silva MD, Germanos MS, Bolen JB, Claiborne CF, Sells TB. Characterization of Alisertib (MLN8237), an investigational small-molecule inhibitor of aurora A kinase using novel in vivo pharmacodynamic assays. Clin Cancer Res. 17:7614–7624.2011; [PubMed: 22016509]
28. Yang H, Lawrence HR, Kazi A, Gevariya H, Patel R, Luo Y, Rix U, Schonbrunn E, Lawrence NJ, Sebti SM. Dual Aurora A and JAK2 kinase blockade effectively suppresses malignant transformation. Oncotarget. 5:2947–2961.2014; [PubMed: 24930769]
29. Chou TC. Theoretical basis, experimental design, and computerized simulation of synergism and antagonism in drug combination studies. Pharmacol Rev. 58:621–681.2006; [PubMed: 16968952]
30. Lawrence HR, Martin MP, Luo Y, Pireddu R, Yang H, Gevariya H, Ozcan S, Zhu JY, Kendig R, Rodriguez M, Elias R, Cheng JQ, Sebti SM, Schonbrunn E, Lawrence NJ. Development of *o*-chlorophenyl substituted pyrimidines as exceptionally potent aurora kinase inhibitors. J Med Chem. 55:7392–7416.2012; [PubMed: 22803810]
31. de Groot CO, Hsia JE, Anzola JV, Motamedi A, Yoon M, Wong YL, Jenkins D, Lee HJ, Martinez MB, Davis RL, Gahman TC, Desai A, Shiau AK. A cell biologist's field guide to aurora kinase inhibitors. Front Oncol. 5:285.2015; [PubMed: 26732741]
32. Heninger AK, Theil A, Wilhelm C, Petzold C, Huebel N, Kretschmer K, Bonifacio E, Monti P. IL-7 abrogates suppressive activity of human $CD4^+CD25^+FOXP3^+$ regulatory T cells and allows expansion of alloreactive and autoreactive T cells. J Immunol. 189:5649–5658.2012; [PubMed: 23129754]
33. Samarasinghe S, Mancao C, Pule M, Nawroly N, Karlsson H, Brewin J, Openshaw P, Gaspar HB, Veys P, Amrolia PJ. Functional characterization of alloreactive T cells identifies CD25 and CD71 as optimal targets for a clinically applicable allodepletion strategy. Blood. 115:396–407.2010; [PubMed: 19890093]
34. Touil S, Rosenzwajg M, Landau DA, Le Corvoisier P, Frederic C, Klatzmann D, Maury S, Cohen JL. Depletion of T regulatory cells through selection of CD127-positive cells results in a population enriched in memory T cells: Implications for anti-tumor cell therapy. Haematologica. 97:1678–1685.2012; [PubMed: 22581007]
35. Liu W, Putnam AL, Xu-yu Z, Szot GL, Lee MR, Zhu S, Gottlieb PA, Kapranov P, Gingeras TR, de St Groth BF, Clayberger C, Soper DM, Ziegler SF, Bluestone JA. CD127 expression inversely correlates with FoxP3 and suppressive function of human $CD4^+$ T reg cells. J Exp Med. 203:1701–1711.2006; [PubMed: 16818678]
36. Seddiki N, Santner-Nanan B, Martinson J, Zaunders J, Sasson S, Landay A, Solomon M, Selby W, Alexander SI, Nanan R, Kelleher A, de StGroth BF. Expression of interleukin (IL)-2 and IL-7 receptors discriminates between human regulatory and activated T cells. J Exp Med. 203:1693–1700.2006; [PubMed: 16818676]
37. Mandapathil M, Hilldorfer B, Szczepanski MJ, Czystowska M, Szajnik M, Ren J, Lang S, Jackson EK, Gorelik E, Whiteside TL. Generation and accumulation of immunosuppressive adenosine by human $CD4^+CD25highFOXP3^+$ regulatory T cells. J Biol Chem. 285:7176–7186.2010; [PubMed: 19858205]
38. Wilson J, Cullup H, Lourie R, Sheng Y, Palkova A, Radford KJ, Dickinson AM, Rice AM, Hart DN, Munster DJ. Antibody to the dendritic cell surface activation antigen CD83 prevents acute graft-versus-host disease. J Exp Med. 206:387–398.2009; [PubMed: 19171763]
39. Seldon TA, Pryor R, Palkova A, Jones ML, Verma ND, Findova M, Braet K, Sheng Y, Fan Y, Zhou EY, Marks JD, Munro T, Mahler SM, Barnard RT, Fromm PD, Silveira PA, Elgundi Z, Ju X, Clark GJ, Bradstock KF, Munster DJ, Hart DNJ. Immunosuppressive human anti-CD83 monoclonal antibody depletion of activated dendritic cells in transplantation. Leukemia. 30:692–700.2016; [PubMed: 26286117]
40. Blagih J, Coulombe F, Vincent EE, Dupuy F, Galicia-Vázquez G, Yurchenko E, Raissi TC, van der Windt GJ, Viollet B, Pearce EL, Pelletier J, Piccirillo CA, Krawczyk CM, Divangahi M, Jones RG. The energy sensor AMPK regulates T cell metabolic adaptation and effector responses in vivo. Immunity. 42:41–54.2015; [PubMed: 25607458]

41. Peres RS, Liew FY, Talbot J, Carregaro V, Oliveira RD, Almeida SL, França RF, Donate PB, Pinto LG, Ferreira FI, Costa DL, Demarque DP, Gouvea DR, Lopes NP, Queiroz RHC, Silva JS, Figueiredo F, Alves-Filho JC, Cunha TM, Ferreira SH, Louzada-Junior P, Cunha FQ. Low expression of CD39 on regulatory T cells as a biomarker for resistance to methotrexate therapy in rheumatoid arthritis. Proc Natl Acad Sci USA. 112:2509–2514.2015; [PubMed: 25675517]

42. Thiolat A, Semerano L, Pers YM, Biton J, Lemeiter D, Portales P, Quentin J, Jorgensen C, Decker P, Boissier MC, Louis-Plence P, Bessis N. Interleukin-6 receptor blockade enhances $CD39^{+}$ regulatory T cell development in rheumatoid arthritis and in experimental arthritis. Arthritis Rheumatol. 66:273–283.2014; [PubMed: 24504799]

43. Pasquini MC, Devine S, Mendizabal A, Baden LR, Wingard JR, Lazarus HM, Appelbaum FR, Keever-Taylor CA, Horowitz MM, Carter S, O'Reilly RJ, Soiffer RJ. Comparative outcomes of donor graft $CD34^{+}$ selection and immune suppressive therapy as graft-versus-host disease prophylaxis for patients with acute myeloid leukemia in complete remission undergoing HLA-matched sibling allogeneic hematopoietic cell transplantation. J Clin Oncol. 30:3194–3201.2012; [PubMed: 22869882]

44. Kanakry CG, Tsai HL, Bolaños-Meade J, Smith BD, Gojo I, Kanakry JA, Kasamon YL, Gladstone DE, Matsui W, Borrello I, Huff CA, Swinnen LJ, Powell JD, Pratz KW, DeZern AE, Showel MM, McDevitt MA, Brodsky RA, Levis MJ, Ambinder RF, Fuchs EJ, Rosner GL, Jones RJ, Luznik L. Single-agent GVHD prophylaxis with posttransplantation cyclophosphamide after myeloablative, HLA-matched BMT for AML, ALL, and MDS. Blood. 124:3817–3827.2014; [PubMed: 25316679]

45. Cooke KR, Kobzik L, Martin TR, Brewer J, Delmonte J Jr, Crawford JM, Ferrara JL. An experimental model of idiopathic pneumonia syndrome after bone marrow transplantation: I. The roles of minor H antigens and endotoxin. Blood. 88:3230–3239.1996; [PubMed: 8963063]

46. Neri S, Mariani E, Meneghetti A, Cattini L, Facchini A. Calcein-acetyoxymethyl cytotoxicity assay: Standardization of a method allowing additional analyses on recovered effector cells and supernatants. Clin Diagn Lab Immunol. 8:1131–1135.2001; [PubMed: 11687452]

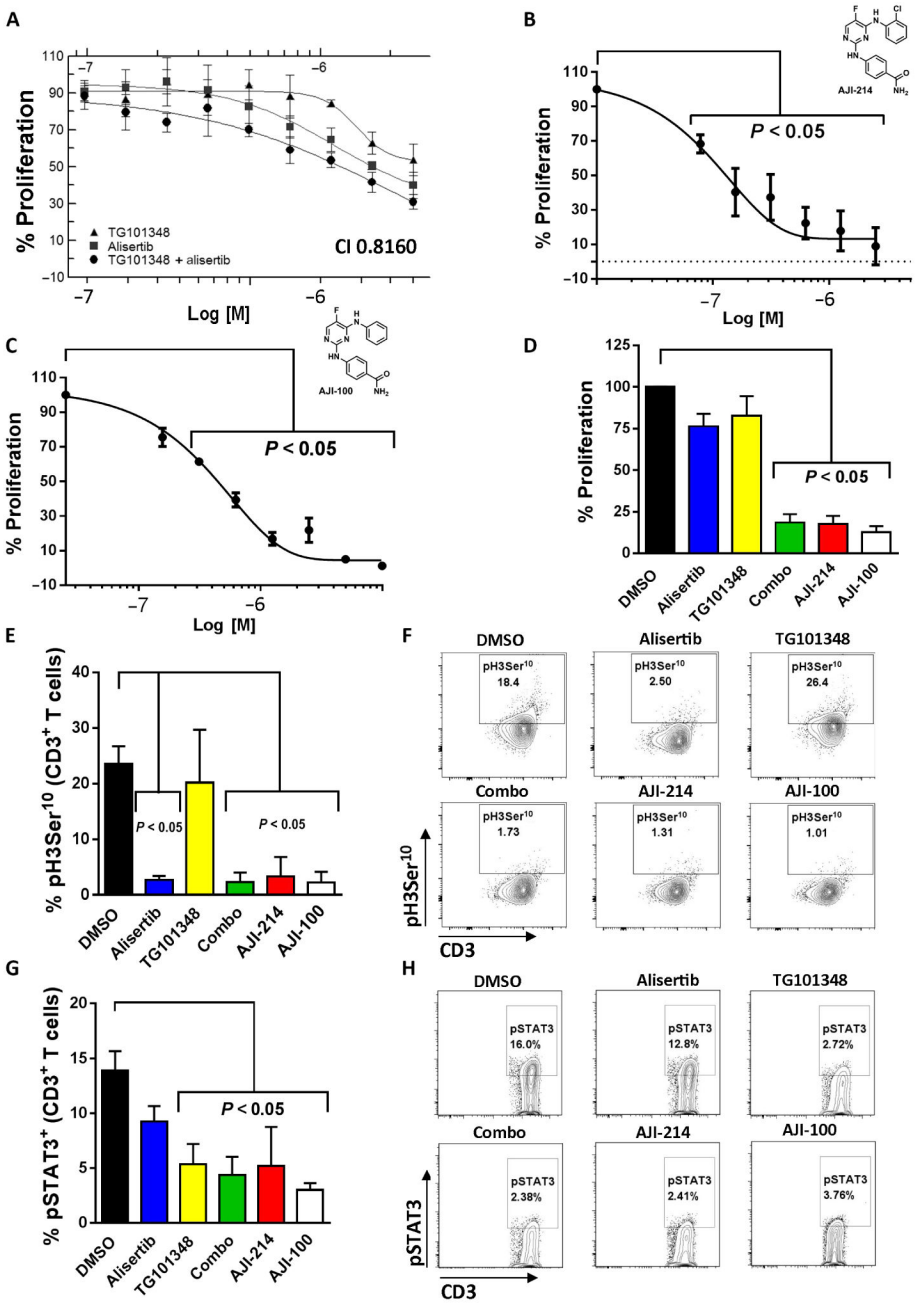

Fig. 1. Synergistic immunosuppression with combined inhibition of Aurora kinase A and JAK2

(**A**) Human T cells were stimulated with DCs (DC/T cell ratio of 1:30) exposed to TG101348 (JAK2 inhibitor), alisertib (Aurora kinase A inhibitor), or both TG101348 and alisertib at a fixed ratio of 1:5, respectively, at varying concentrations once on day 0. Proliferation was determined by fluorescence assay on day 5, with % proliferation based on dimethyl sulfoxide (DMSO) control. Graph depicts combination synergy (IC_{50} values for TG101348 and alisertib were 350 nM and 1.75 μM, respectively), showing one representative independent experiment of two performed with triplicate technical replicates. The CI was calculated using the Chou-Talalay method. AlloMLR (DC/T cell ratio of 1:30)

treated with AJI-214 (**B**), AJI-100 (**C**) (dual JAK2/Aurora kinase A inhibitors), or DMSO once on day 0 is shown. IC_{50} values for AJI-214 and AJI-100 were 100 and 200 nM, respectively. Graph shows average triplicate means ± SEM from two to three independent experiments [analysis of variance (ANOVA)]. (**D**) Bar graph depicts T cell proliferation when exposed to alisertib (1.75 μM), TG101348 (350 nM), a combination of alisertib and TG101348 (combo), AJI-214 (750 nM), or AJI-100 (750 nM) in alloMLRs. Means ± SEM from four independent experiments (ANOVA) are shown using triplicate technical replicates. (**E** to **H**) Bar graphs depict the mean gated $CD3^+$ T cell $H3Ser^{10}$ (target of Aurora) or STAT3 (target of JAK2) phosphorylation ± SD from three independent experiments after stimulation with allogeneic DCs (5 days) or IL-6 (15 min), respectively (ANOVA). Representative contour plots show $H3Ser^{10}$ and STAT3 phosphorylation, respectively.

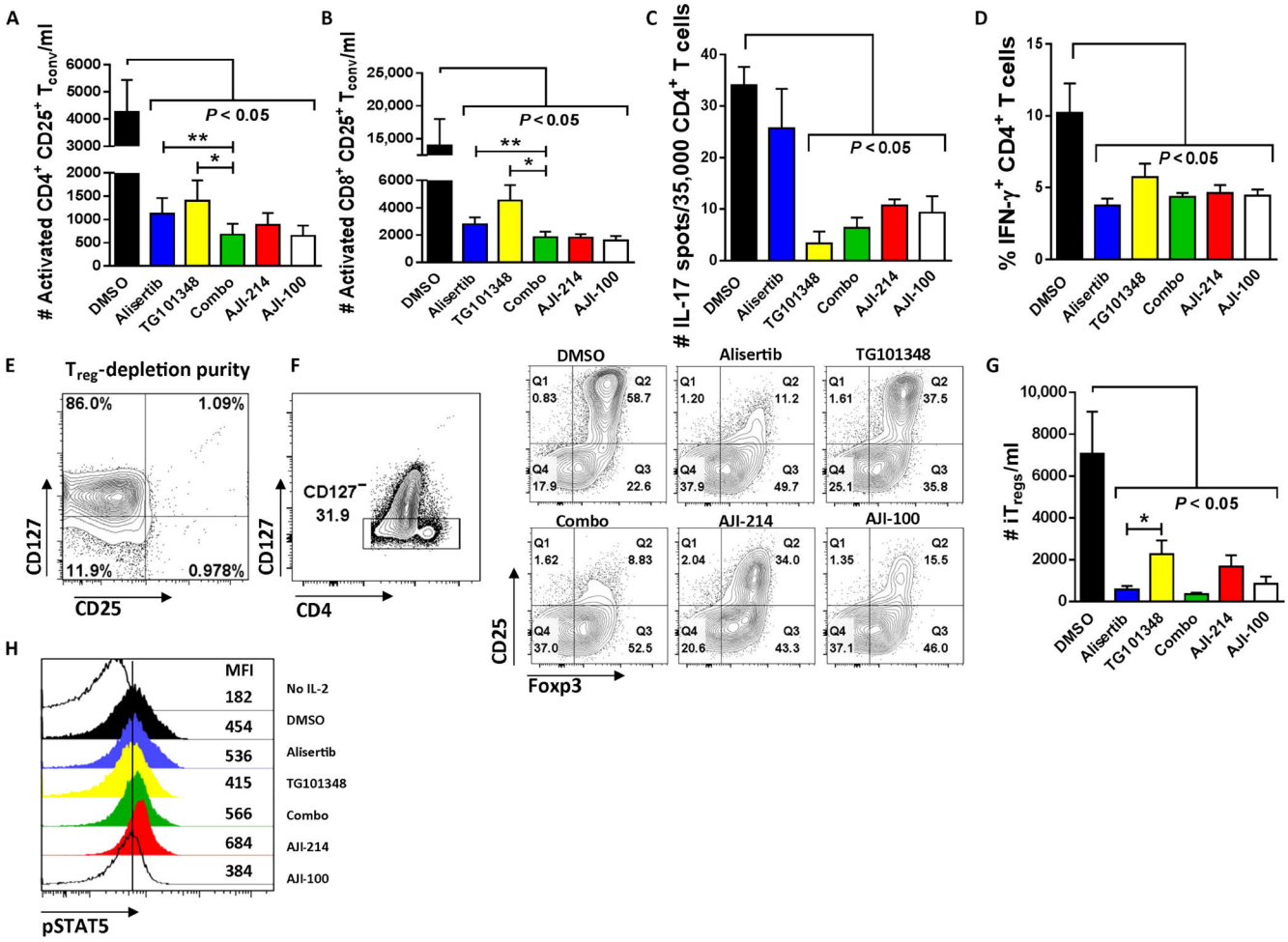

Fig. 2. Immunosuppressive effect of Aurora kinase A/JAK2 blockade on responder T_{conv} and T_H subsets

(**A** and **B**) T cells were stimulated with allogeneic DCs (DC/T cell ratio of 1:30) and treated with kinase inhibitors or DMSO once on day 0. Bar graphs show replicate mean absolute numbers of activated $CD4^+$, $CD25^+$, $CD127^+$ or activated $CD8^+$, $CD25^+$ T_{conv} ± SEM at day +5 from six independent experiments (ANOVA and paired *t* test). (**C**) Bar graph shows the mean number of IL-17 spots per well ± SD from triplicate technical replicates among DC-allostimulated $CD4^+$ T cells. One of three representative experiments is shown. (**D**) Bar graph shows mean % $CD4^+$, IFN-γ^+ T cells ± SEM at day +5 of alloMLR from five independent experiments with technical replicates performed in triplicate. (**E** and **F**) Representative contour plots show T_{reg} ($CD25^+$ and $CD127^-$) depletion of $CD4^+$ T cell responders at outset of alloMLR (DC/T cell ratio of 1:30), followed by induction of iT_{reg} ($CD127^-$, $CD25^+$, and $Foxp3^+$) after 5 days of culture exposed to kinase inhibitors or DMSO. (**G**) Bar graph shows mean absolute numbers of iT_{regs} ± SEM from seven independent experiments performed with two to three technical replicates (ANOVA and paired *t* test). (**H**) Representative histograms depict pSTAT5 expression among IL-2–stimulated $CD3^+$ T cells while exposed to kinase inhibitors or DMSO. Geometric mean fluorescence intensity (MFI) of pSTAT5 is shown along the right margin. One of three

representative experiments is shown. *$P < 0.05$, **$P = 0.001$ to 0.01. Alisertib (1.75 μM), TG101348 (350 nM), AJI-214 (750 nM), and AJI-100 (750 nM).

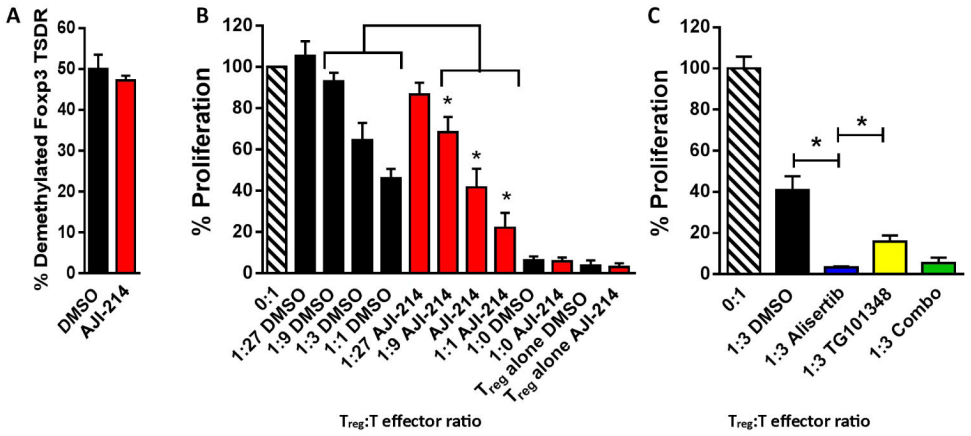

Fig. 3. Combined inhibition of Aurora kinase A and JAK2 enhances antigen-specific iT_{reg}-suppressive potency

(**A**) Bar graph depicts mean % demethylation of Foxp3 ± SEM among iT_{regs} in alloMLRs treated with AJI-214 (750 nM) or DMSO from four independent experiments using triplicate technical replicates. (**B**) The suppressive capacity of sorted, DC-allostimulated iT_{regs} previously exposed to AJI-214 or DMSO was tested at different ratios of iT_{reg} to T cell responders stimulated by fresh allogeneic DCs (DC/responder T cell ratio of 1:30) in alloMLRs. No additional AJI-214 or DMSO was added. Bar graph shows means of % proliferation ± SEM based on [^{3}H]thymidine incorporation on day 6 from three independent experiments with triplicate technical replicates (ANOVA). (**C**) The potency of iT_{regs} generated in the presence of alisertib (1.75 μM), TG101348 (350 nM), a combination of alisertib and TG101348, or DMSO was tested in standard suppression assays. No additional small-molecule inhibitors or DMSO was added. Bar graph shows means of % proliferation ± SD based on [^{3}H]thymidine incorporation on day 6 (paired *t* test). Data are from one representative experiment of two performed using triplicate technical replicates. *$P < 0.05$.

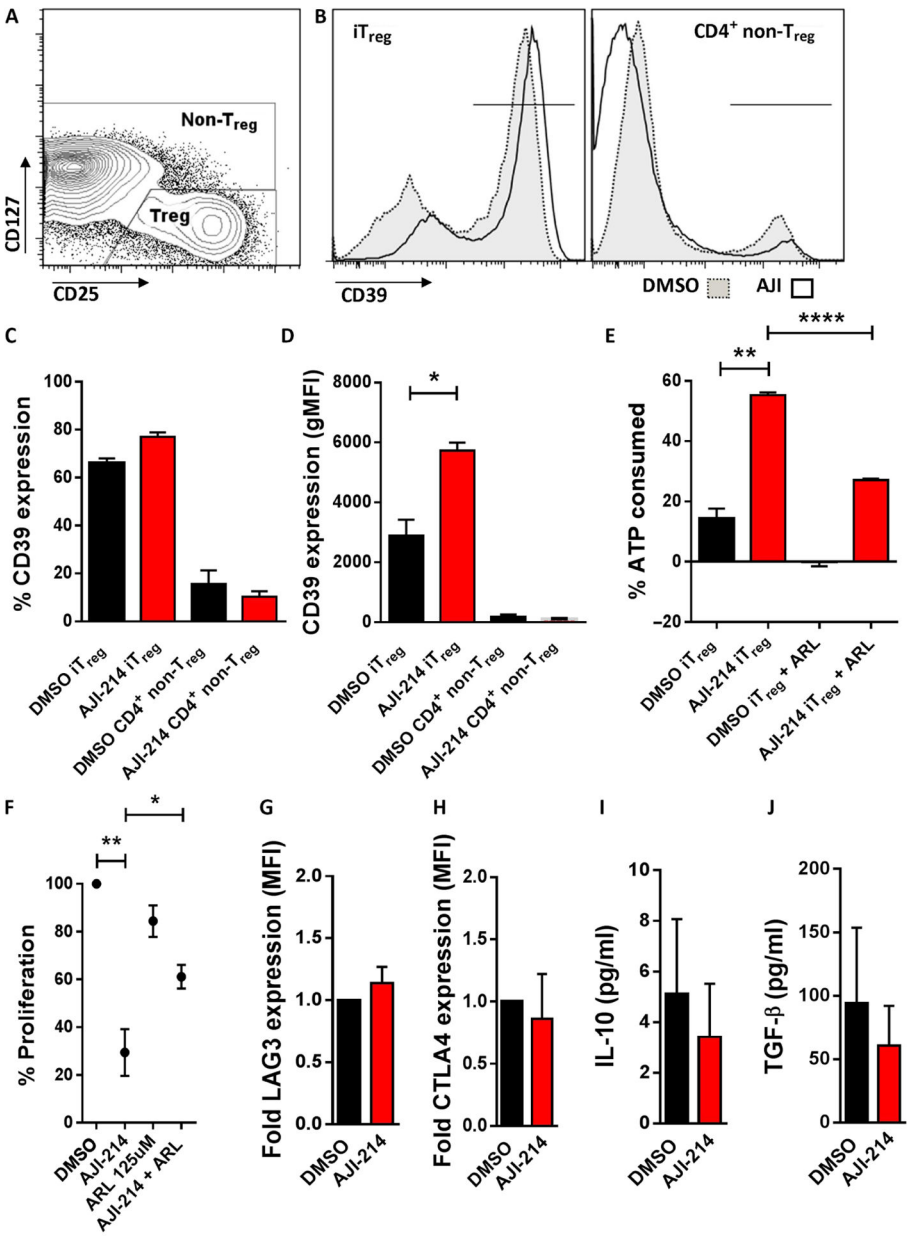

Fig. 4. Targeting Aurora kinase A and JAK2 increases CD39 expression and ATP scavenging among iT$_{reg}$

(**A**) Contour plots show the CD4$^+$ iT$_{reg}$ and non-T$_{reg}$ gating strategy after 5-day alloMLR treated with AJI-214 (750 nM) or DMSO. (**B** to **D**) CD39 density [geometric MFI (gMFI)] is increased by among iT$_{reg}$ generated in the presence of AJI-214 (750 nM). Bar graphs show mean data ± SD from three independent experiments (paired *t* test). (**E**) Bar graphs show replicate means of ATP consumption ± SD after stimulating 75,000 iT$_{regs}$ with 50 μM ATP for 45 min. ATP was measured by luminescence assay. Data are from one representative experiment of two performed using triplicate technical replicates (paired *t* test). (**F**) AlloMLRs of naïve, T$_{reg}$-depleted CD4$^+$ T cells and allogeneic DCs (DC/T cell ratio of 1:30) were treated with AJI-214, ARL67156 (CD39 inhibitor), both AJI-214 and

ARL67156, or DMSO. Proliferation was determined by colorimetric assay on day 5, with % proliferation based on DMSO control. Graph shows means ± SEM from five independent experiments using three technical replicates (paired *t* test). (**G** and **H**) Bar graphs depict mean fold MFI of LAG3 and CTLA4 ± SD on iT_{regs} harvested from alloMLRs treated with AJI-214 or DMSO from three independent experiments. (**I** and **J**) Bar graphs show mean concentrations of IL-10 and TGF-β ± SEM among PMA (phorbol 12-myristate 13-acetate)/ionomycin–stimulated iT_{regs} previously exposed to AJI-214 or DMSO during coculture from four independent experiments using three technical replicates. **P* < 0.05, ***P* = 0.001 to 0.01, *****P* < 0.0001.

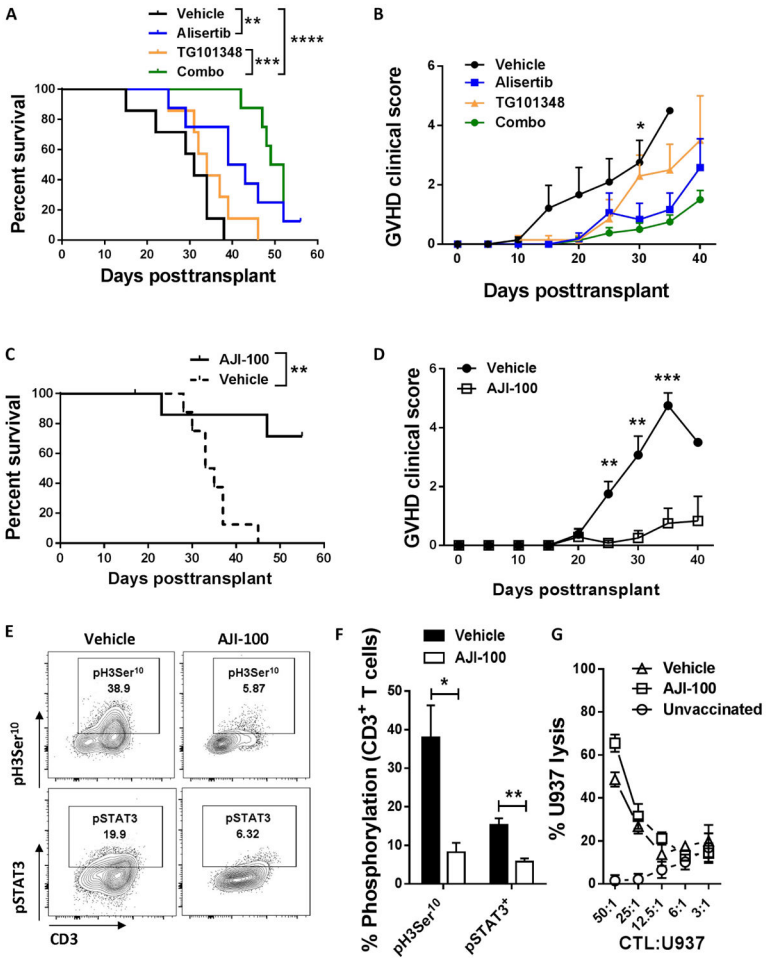

Fig. 5. Blockade of Aurora kinase A and JAK2 reduces xenogeneic GVHD and preserves the in vivo generation of potent antitumor CTL

NSG mice received human PBMCs (30×10^6 cells) by intraperitoneal injection, with alisertib (30 mg/kg daily), TG101348 (45 mg/kg twice a day), a combination of alisertib and TG101348, or vehicle administered by oral gavage from day 0 to day +14. (**A**) Percent survival is shown among the four groups (log-rank test). (**B**) Graph shows mean GVHD clinical scores ± SEM for each group of mice ($P = 0.02$ at day +30, vehicle versus combo, Mann-Whitney). Pooled data are from two independent experiments. $n = 7$ to 8 mice per group. NSG mice were transplanted with human PBMCs as described, with AJI-100 (50 mg/kg daily) or vehicle administered ip from day 0 to day +14. (**C** and **D**) Percent survival (log-rank test) and mean GVHD clinical scores ± SEM (Mann-Whitney) are demonstrated. Pooled data are from two independent experiments. $n = 8$ mice per group. (**E**) Representative contour plots show expression of $H3Ser^{10}$ and STAT3 phosphorylation among human $CD3^+$ T cells harvested from recipient spleens at day +14. (**F**) Bar graph shows the mean % $pH3Ser^{10+}$ and % $pSTAT3^+$ T cells ± SEM among AJI-100–treated and vehicle-treated mice at day +14 ($n = 6$ mice per group, two independent experiments, Mann-Whitney). (**G**) Graph depicts mean specific lysis ± SD by human $CD8^+$ CTL generated in vivo using NSG mice transplanted with human PBMCs and vaccinated with irradiated U937cells (1×10^7) on days 0 and +7. Results shown are from one of two independent

experiments, using a total of seven mice per group. U937 lysis was measured by released fluorescence after 4 hours (vehicle versus AJI-100, not significant, Mann-Whitney). *$P <$ 0.05, **$P =$ 0.001 to 0.01, ***$P =$ 0.0001 to 0.001, ****$P <$ 0.0001.

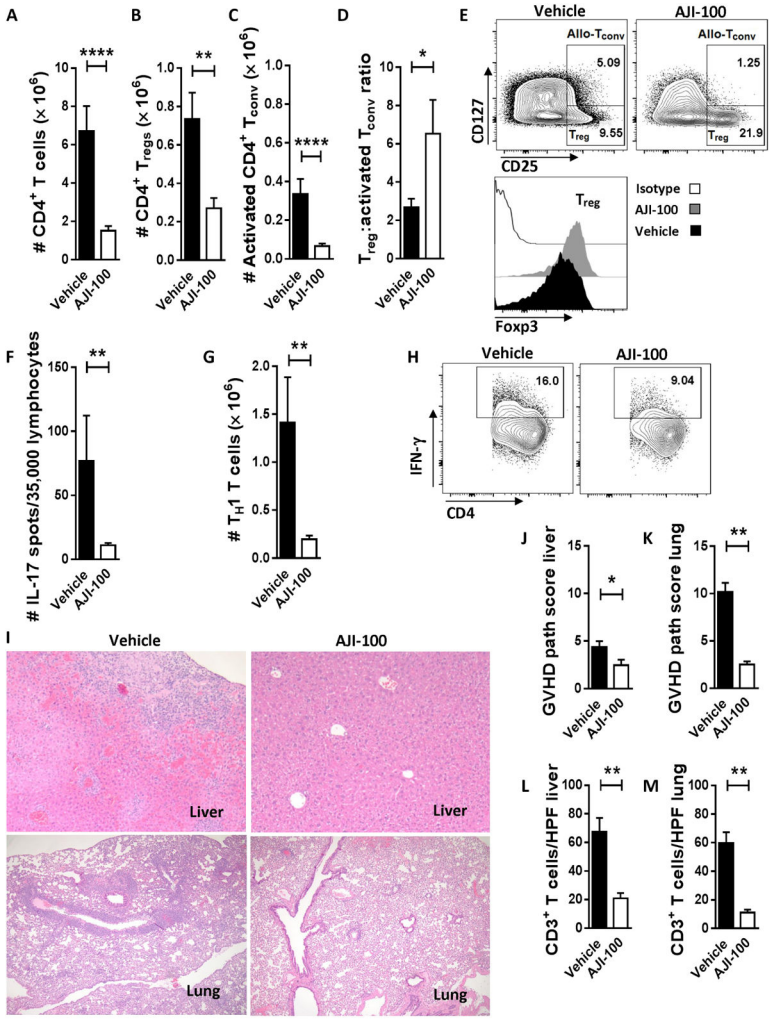

Fig. 6. Targeting Aurora kinase A and JAK2 increases the proportion of T_{reg} to activated T_{conv} and reduces T_H17 and T_H1 cells in xenotransplanted recipient mice

(**A** to **D**) Xenotransplanted NSG mice were treated with AJI-100 (50 mg/kg) or vehicle daily starting at day 0 and then euthanized on day +14. Recipient spleens, livers, and lungs were harvested, and tissue-resident T cells were evaluated. Bar graphs show replicate mean absolute number of human $CD4^+$ T cells (A), $CD4^+$ T_{regs} (B), $CD4^+$ activated T_{conv} ($CD25^+$ and $CD127^+$) (C), and the ratio of T_{reg} to activated T_{conv} (D) ± SEM (Mann-Whitney). (**E**) Representative contour plots show the % $CD4^+$ T_{reg} and % $CD4^+$ activated allo-T_{conv} residing in spleens of AJI-100–treated or vehicle-treated mice at day +14. The representative histograms show corresponding expression of Foxp3 within the $CD4^+$ T_{regs}. (**F**) Bar graph shows the replicate mean number of IL-17 spots per well ± SEM among human lymphocytes harvested from recipient spleens at day +14 (Mann-Whitney). (**G** and **H**) Bar graph and representative contour plots depict the amount of $CD4^+$, IFN-γ^+ T cells ± SEM from AJI-100 or vehicle-treated mice at day +14 (Mann-Whitney). (**I**) Sections of recipient livers (top) and lung (bottom) show that AJI-100 significantly reduces GVHD damage in recipient target organs, compared to vehicle control. (**J** and **K**) Bar graphs depict the mean GVHD pathology scores ± SEM for host liver and lung at day +14. (**L** and **M**) Bar graphs shows

that the mean number of human $CD3^+$ T cells ± SEM [per high-power field (HPF)] infiltrating liver or lung at day +14 is significantly reduced by AJI-100 compared to vehicle (Mann-Whitney). Pooled data are from at least two independent experiments. $n = 6$ to 14 mice per group. *$P < 0.05$, **$P = 0.001$ to 0.01, ****$P < 0.0001$.